

DMD #72744

**Midostaurin, a Novel Protein Kinase Inhibitor for the Treatment of  
Acute Myelogenous Leukemia: Insights from Human Absorption,  
Metabolism and Excretion Studies of a BDDCS II Drug**

Handan He, Phi Tran, Helen Gu, Vivienne Tedesco, Jin Zhang, Wen Lin, Ewa Gatlik,  
Kai Klein, Tycho Heimbach

Department of Drug Metabolism and Pharmacokinetics

Novartis Institutes for Biomedical Research,

One Health Plaza, East Hanover, NJ, USA

DMD #72744

Running title: Absorption, Metabolism and Excretion of Midostaurin in Humans

Corresponding Author:

Handan He, Ph.D.

Pharmacokinetic Sciences, Novartis Institutes for Biomedical Research,

One Health Plaza, East Hanover, NJ 07936, USA

Tel: 862-778-3353

Fax: 973-781-5023

Email: handan.he@novartis.com

Number of words in Abstract = 242

Number of words in Introduction = 442

Number of words in Discussion = 1474

Number of references = 28

Number of text pages = 29

Number of tables = 6

Number of figures = 6

Abbreviations: BCS, Biopharmaceutics Classification System; BDDCS, Biopharmaceutics Drug Disposition Classification System;  $C_{\max}$ , maximum concentration;  $f_u$ , fraction unbound, LC/MS/MS, liquid chromatography-tandem mass

DMD #72744

spectrometry; HPLC, high-performance liquid chromatography; LSC, liquid scintillation counting; PKC, protein kinase C

DMD #72744

**Abstract**

The absorption, metabolism and excretion of midostaurin, a potent class III tyrosine protein kinase inhibitor for acute myelogenous leukemia, were evaluated in healthy subjects. A microemulsion formulation was chosen to optimize absorption. After a 50 mg [ $^{14}\text{C}$ ]midostaurin dose, oral absorption was high (> 90%) and relatively rapid. In plasma, the major circulating components were midostaurin (22%), CGP52421 (32.7%), and CGP62221 (27.7%). Long plasma half-lives were observed for midostaurin (20.3 h), CGP52421 (495 h), and CGP62221 (33.4 h). Through careful mass-balance study design, the recovery achieved was good (81.6%), despite the long radioactivity half-lives. Most of the radioactive dose was recovered in feces (77.6%) mainly as metabolites; as only 3.43% was unchanged, suggesting mainly hepatic metabolism. Renal elimination was minor (4%). Midostaurin metabolism pathways involved hydroxylation, *O*-demethylation, amide hydrolysis and *N*-demethylation. High plasma CGP52421 and CGP62221 exposures in humans, along with relatively potent cell-based IC<sub>50</sub> for FLT3-ITD inhibition, suggested that the antileukemic activity in AML patients may also be maintained by the metabolites. Very high plasma protein binding (>99%) required equilibrium gel filtration to identify differences between humans and animals. As midostaurin, CGP52421 and CGP62221 are metabolized mainly by CYP3A4 and are inhibitors/inducers for CYP3A, potential drug-drug interactions with mainly CYP3A4 modulators/CYP3A substrates could be expected. Given its low aqueous solubility, high oral absorption and extensive metabolism (> 90%), midostaurin is a BCS/BDDCS class II drug in human, consistent with rat BDDCS in vivo data showing high absorption (>90%) and extensive metabolism (>90%).

## Introduction

Acute myeloid leukemias (AML) are a heterogeneous group of diseases characterized by infiltration of blood, bone marrow, and other tissues by neoplastic cells of the hematopoietic system (Udayakumar et al. 2006). Approximately two-thirds of adults with AML attain complete remission status following induction therapy; however the remission is often not durable with about 25% of those whom attained complete remission surviving three or more years. Therefore, novel therapeutic strategies are needed to improve prognosis (Furukawa et al. 2007; Lowenberg et al., 1999; Hatcher et al., 2016). The FMS-like tyrosine kinase 3 (FLT3) is a member of class III receptor tyrosine kinases, and structurally related to c-kit, c-FMS and platelet-derived growth factor-receptor (PDGF-R) tyrosine kinases (Rosnet et al., 1991). FLT3 is expressed by immature hematopoietic cells and is important for the normal development of stem cells and the immune system. FLT3 receptor is detectably expressed in >80 % of patients with AML, either as mutant FLT3 forms, or as overexpressed (increased mRNA) WT FLT3 (Birg et al., 1992). FLT3 mutations have been shown to have oncogenic potential (Weisberg et al., 2002). There are two kinds of FLT3 mutations reported in AML; internal tandem duplications (ITD) and point mutations. Constitutive activation of FLT3 via internal tandem duplication is the most common mutation that is found in 35% of patients with AML, and it is generally correlated with poor prognosis (Kiyoi et al., 1999; Kottaridis et al., 2001; Thiede et al., 2002; Yanada et al., 2005). FLT3 tyrosine kinase inhibitors are emerging as the most promising drug therapy to overcome the dismal prognosis of AML patients harboring internal tandem duplication of FLT3 (Breitenbuecher et al. 2009). Midostaurin (*N*-benzoyl-staurosporine), a potent inhibitor of

## DMD #72744

mutant FLT3 (Fabbro et al., 2000), is being developed as an antileukemia agent in AML patients with mutant FLT3 receptors. Midostaurin induces cell cycle arrest and apoptosis in leukemic cells expressing FLT3 mutant receptors (Weisberg et al., 2002). Midostaurin has hematologic activity in patients with wild type and mutant FLT3 (Fischer et al., 2010) and is the first oral FLT-3 inhibitor to offer an extended survival for patients with FLT-3 mutated AML in combination with other standard chemotherapy (Stone, 2016). To date, midostaurin has shown good tolerability among patients in the completed clinical trials. Based primarily on the Phase III RATIFY clinical study, the United States Food and Drug Administration (FDA) granted Breakthrough Therapy designation to PKC412 (midostaurin) in February 2016 (Novartis, 2016). To facilitate drug approval, mass balance studies are typically conducted during late drug development stages (Lin et al. 2012, Penner et al. 2012). Here insights from absorption, metabolism and excretion studies conducted with midostaurin, a highly lipophilic drug, are described.

## Materials and Methods

**Study drug:** [ $^{14}\text{C}$ ]Midostaurin; specific activity 2  $\mu\text{Ci}/\text{mg}$ , radiochemical purity  $\geq 98\%$ ) was synthesized by the Isotope Laboratory of Novartis Pharmaceuticals Corporation (Basel, Switzerland). Synthetic standards CGP52421 (epimers 1 and 2), CGP62221, [ $^{13}\text{C}_6$ ]midostaurin, [ $^{13}\text{C}_6$ ]CGP52421 (epimers 1 and 2) and [ $^{13}\text{C}_6$ ]CGP62221 used as internal standards for the analysis of unchanged midostaurin were synthesized by Novartis Pharmaceuticals Corporation. Benzoic acid and hippuric acid were purchased from Sigma-Aldrich (USA). The chemical structures of radiolabeled midostaurin, the position of the radiolabel along with related compounds are shown in Figure 1.

**Human studies:** The study protocol and the informed consent document were approved by an independent institutional review board. The written informed consent was obtained from the subjects before enrollment.

Six healthy subjects included five males and one female from 22 to 51 years of age, with weights ranging from 66.8-80.5 kg, participated in the study. Subjects were confined to the study center for at least 24 hours before administration of study drug until 168 hours (7 days) post-dose. After a fast of at least 10 h, the subjects were given a single oral dose of 50 mg of [ $^{14}\text{C}$ ]midostaurin formulated as a microemulsion drink solution containing Cremophor RH40 (polyoxyl hydrogenated castor oil), corn oil glycerides, propylene glycol and ethanol. The radioactive dose given per subject was 100  $\mu\text{Ci}$  based on dosimetry assessments and approved by the radiation safety committee. After administration, the volunteers continued to abstain from food for an additional 4 h.

## DMD #72744

For the quantitation of midostaurin and its metabolites CGP52421 and CGP62221 in plasma, blood was collected pre-dose and at 0.5, 1, 2, 3, 4, 6, 8, 12, 24, 48, 72, 96, 120, 144, 168, 252, 336, 504, 864, 1344, and 2016 h post-dose by an indwelling cannula inserted in a forearm vein. Venous blood (4mL) was collected at each time point in heparinized tubes. Plasma was separated from whole blood by centrifugation, transferred to a screw-top polypropylene tube, and immediately frozen. For the determination of radioactivity in blood and plasma and for metabolite profiling, blood was collected for analysis at the same time points out to 168 h post-dose. Urine samples were collected at pre-dose, 0 to 8, 8 to 24, 24 to 48, 48 to 72, 72 to 96, 96 to 120, 120 to 144, and 144 to 168 h post-dose. Feces were collected continuously through day 8 and spot fecal samples were obtained on days 9, 13, 20, and 83. All samples were stored at  $\leq -18^{\circ}\text{C}$  until analysis.

**Radioactivity Analysis of Blood, Plasma, Urine, and Feces Samples:** Radioactivity was measured in plasma, blood, urine, and feces by liquid scintillation counting (LSC). Plasma and urine were mixed with liquid scintillant and counted directly; whole blood samples were mixed with liquid scintillant after digestion with tissue solubilizer (Soluene 350<sup>®</sup>), decolorization was performed using hydrogen peroxide, and stored in the dark to reduce luminescence. Fecal samples were homogenized in water and aliquots were combusted with a biological oxidizer prior to LSC.

The radioactivity in the dose was defined as 100% of the total radioactivity. The radioactivity at each sampling time for urine and feces was defined as the percentage of dose excreted in the respective matrices. The radioactivity measured in plasma was



## DMD #72744

converted to nanogram-equivalents of midostaurin based on the specific activity of the dose.

### **Analysis of Unchanged Midostaurin and Metabolites CGP62221 and CGP52421**

Unchanged midostaurin and its metabolites CGP62221 and CGP52421 (epimers 1 and 2) were measured quantitatively in plasma using a previously validated LC/MS/MS assay. Liquid-liquid extraction of the samples was performed by adding 2 ml of tertbutylmethylether to glass tubes containing aliquots of plasma (100  $\mu$ L), along with 100  $\mu$ L water and 50  $\mu$ L of internal standard (IS) solution. After vortexing and centrifugation (5°C, 3000 rpm) the glass tubes were placed on dry ice and the organic phase was transferred to new glass tubes. After evaporation of the extracts to dryness under nitrogen at 40°C, 200  $\mu$ L of acetonitrile-water (50:50, v/v) was added and the tubes were vortex-mixed. For analysis, aliquots (10  $\mu$ L) of the extracts were injected onto the HPLC system.

For the quantitation of midostaurin and its metabolite CGP62221, the HPLC system consisted of a Series 200 pump and autosampler (PerkinElmer Life Sciences Inc). The column was a Symmetry C<sub>18</sub> (50 x 2.1 mm, 3.5 $\mu$ m) (Waters, Milford, MA) maintained at room temperature. A gradient elution was used and the mobile phase consisted of 5 mM ammonium acetate (solvent A) and acetonitrile (solvent B). The mobile phase was initially composed of solvent A/solvent B (55:45); the gradient was then linearly programmed to solvent A/solvent B (40:60) over 4 min and held for 0.5 min; to solvent A/solvent B (55:45) over 1 min and held for 1 min. The flow rate was maintained at 0.25 mL/min. The HPLC system was interfaced to a Sciex API 3000 triple quadrupole mass spectrometer (Applied Biosystems/MDS Sciex, Concord, ON, Canada) that was operated

## DMD #72744

in the positive ion electrospray ionization mode. For multiple reaction monitoring, the transitions monitored were  $m/z$  571  $\rightarrow$   $m/z$  348 for midostaurin,  $m/z$  577  $\rightarrow$   $m/z$  348 for the IS ( $[^{13}\text{C}_6]$  midostaurin),  $m/z$  557  $\rightarrow$   $m/z$  348 for CGP62221 and  $m/z$  563  $\rightarrow$   $m/z$  348 for the IS ( $[^{13}\text{C}_6]$  CGP62221). MS temperature: 450°C; dwell time: 500 msec; collision energy: 33eV. For both analytes, the dynamic range of the assay was 10.0 to 5000 ng/mL.

For the quantitation of metabolite CGP52421 (epimers 1 and 2), the HPLC system consisted of an Agilent Series 1100 pump (Agilent Technologies, CA) and a CTC Analytics HTS PAL autosampler (Leap Technologies, Carrboro, NC). The column used was an Alltima C<sub>18</sub> (50 x 2.1 mm, 5 $\mu$ m) (Alltech). The mobile phase flow rate was 0.25 mL/min, and the column temperature was maintained at 60°C. The components were eluted from the column with an isocratic solvent system (33% solvent A and 67% solvent B). The HPLC system was interfaced to a TSQ 7000 API II triple quadrupole mass spectrometer (Thermo Fisher Scientific, Waltham, MA) that was operated in the positive ion electrospray ionization mode. For multiple reaction monitoring, the transitions monitored were  $m/z$  587  $\rightarrow$   $m/z$  364 for CGP52421 and  $m/z$  593  $\rightarrow$   $m/z$  364 for the IS ( $[^{13}\text{C}_6]$  CGP52421). The MS temperature: 340°C; dwell time, 500 msec; collision energy, 25eV. The dynamic range of the assay was from 20.0 to 2000 ng/mL.

**Sample Preparation of Plasma, Urine, and Feces for Metabolite Investigation.** Semi-quantitative determination of main and trace metabolites was performed by radio-HPLC with off-line microplate solid scintillation counting and structural characterization by LC-MS.

Plasma samples (1.2 ml) from each subject at 0.5, 1, 4, 8, 24, 48, 72, and 96 h post-dose were protein precipitated with acetonitrile:ethanol (90:10 v/v) and removed by

## DMD #72744

centrifugation. Recoveries of radioactivity averaged 90%. The supernatant was evaporated to near dryness under a stream of nitrogen using the Zymark turbo-vap LV (Zymark Corp., Hopkinton, MA), and the residues were reconstituted in 120  $\mu$ l methanol:water (75:25). Urine was pooled from 0 to 72 h, accounting for >90% of the excreted dose and was proportional to the volume of urine collected at each time point. An aliquot of the pooled urine was concentrated approximately 5-fold by reducing the sample volume under a gentle stream of nitrogen and centrifuged. Feces homogenates were pooled (from 0 to 144 h) on a weight basis to account for >90% radioactivity. Each pooled fecal sample was extracted twice with methanol by vortex-mixing and centrifugation. The average recovery of sample radioactivity in the methanolic extracts was 88%. Aliquots of combined supernatant were evaporated to dryness, reconstituted in methanol:water, and aliquots (40-45  $\mu$ l) of concentrated plasma, urine, feces extracts were injected onto the HPLC system.

**HPLC Instrumentation for Metabolite Pattern Analysis.** Midostaurin and its metabolites in plasma and excreta were analyzed by HPLC with off-line radioactivity detection using a Waters Alliance 2795 HPLC system (Waters, Milford, MA) equipped with a Phenomenex Synergy Max-RP (Phenomenex, Torrance, CA) column (4.6 X 150 mm, 4  $\mu$ m, maintained at 40°C) and a guard column of the same type. The mobile phase consisted of 10 mM ammonium acetate containing 0.1% acetic acid (pH 4.35) (solvent A) and acetonitrile (solvent B). The mobile phase was initially composed of solvent A/solvent B (95:5), and held for 4 min. The mobile phase composition was then linearly programmed to solvent A/solvent B (70:30) over 6 min; to solvent A/solvent B (51:49) over 45 min; to solvent A/solvent B (5:95) over 5 min and held for 5 min. The mobile

## DMD #72744

phase condition was returned to the starting solvent mixture over 0.5 min. Then system was allowed to equilibrate for 10 min prior to the next injection. A flow rate of 1.0 ml/min was used for all analysis. The HPLC effluent was fractionated into a 96 deep-well Lumaplate<sup>TM</sup> (Packard Instrument Company, Meriden, CT) using a fraction collector (FC 204, Gilson Inc., Middleton, WI) with a collection time of 9 sec per well. Samples were dried under a stream of nitrogen, sealed, and counted for 5–20 min per well on a TopCount<sup>®</sup> microplate scintillation counter (Packard Instrument Company).

The amounts of metabolites of parent drug in plasma or excreta were derived from the radio chromatograms (metabolite patterns) by dividing the radioactivity in original sample in proportion to the relative peak areas. Parent drug or metabolites were expressed as concentrations (ng-Equivalent/ml) in plasma or as percentage of dose in excreta. These values are to be considered as semiquantitative only, as opposed to those determined by the validated quantitative LC/MS/MS assay.

**Structural Characterization of Metabolites by LC/MS/MS.** Metabolite characterization was conducted with a Waters two-channel Z-spray (LockSpray<sup>TM</sup>) time-of-flight mass spectrometer (Q-ToF Ultima Global, Manchester, UK). Leucine enkephalin was used as the mass reference standard for exact mass measurement and was delivered via the second spray channel at a flow rate of 10  $\mu$ L/min. The effluent from the HPLC column was split, and about 250  $\mu$ L/min was introduced into the atmospheric ionization source after diverting to waste during the first 4 min of each run to protect the mass spectrometer from nonvolatile salts. The mass spectrometer was operated at a resolution of  $\sim 9000$  m/ $\Delta m_{FWHM}$  with spectra being collected from 200 to 900 amu. The ionization technique employed was positive electrospray. The sprayer voltage was kept at 3200 V

## DMD #72744

and the cone voltage of the ion source was kept at a potential of 60 V. For the TOF MS/MS experiments, collision energies of 17-20 eV were used with argon as the collision gas.

**Protein binding determination in animals and humans:** *In vitro* plasma protein binding of Midostaurin in the rat (Han-Wistar), dog (Beagle) and human was determined by equilibrium gel filtration, a method reported to be more sensitive and reliable for compounds with high protein binding (>99%); detailed methods were previously described (Weiss and Gatlik, 2014).

Briefly, for the analysis of total binding two 5 mL HiTrap desalting columns (GE Healthcare Bio-Sciences AB, Uppsala, Sweden) were used. The columns were equilibrated with PBS containing the radiolabeled compound under investigation at the chosen concentrations for 16–24 h. Equilibration was at 37°C and 0.2–1 mL/min, at least until a stable compound concentration eluted. Total plasma concentrations in the range of 100–45,000 ng/mL were selected. Starting with the lowest concentration, the same two columns were equilibrated consecutively to the different concentrations tested, with an overnight equilibration to a new higher concentration. Plasma samples from different species were injected alternatingly to limit the impact of inter-run variability on the assessment of species differences. For the validation experiments, only one or two concentrations were chosen because concentration dependency was known. Fibrin in plasma was removed by centrifugation for 10 min at 10,000g. As needed, cleared plasma was diluted with PBS, frozen in aliquots, and thawed before injection. Plasma was injected at volumes/dilutions chosen to ensure that a binding equilibrium was achieved on the column (volumes corresponding to 12.5–100  $\mu$ L of undiluted plasma, lower plasma

## DMD #72744

volumes for compounds displaying higher binding). Plasma (30–200  $\mu$ L) was injected into the equilibrated gel filtration column and run at 0.2–0.4 mL/min. The eluate was analyzed for total protein by UV absorption (280 nm) and for total radioactivity in collected fractions by liquid scintillation counting (LSC) in a Packard Tricarb liquid scintillation counter. Fractions were collected in tubes suitable for LSC to avoid transfer steps and potential losses because of adsorption. Drug concentrations were determined by LSC using the respective specific radioactivities.

**Metabolism of Midostaurin by Human Liver Microsomes and by Recombinant Cytochrome P450s.** The metabolism of [ $^{14}$ C]midostaurin and metabolites CGP52421 and CGP62221 were examined in pooled human liver microsomes and in microsomal preparations from baculovirus-infected insect cells expressing recombinant human cytochrome P450 (CYP) enzymes (BD Gentest). The recombinant CYP enzymes examined in this study were CYP1A1, CYP1A2, CYP2A6, CYP2B6, CYP2C8, CYP2C9, CYP2C19, CYP2D6, CYP2E1, CYP3A4 and CYP3A5. Human liver microsomes or recombinant CYP3A4 (0.2 mg microsomal protein/mL) were pre-incubated with [ $^{14}$ C]midostaurin (0.25–10  $\mu$ M, 1% final methanol concentration, v/v) in 100 mM potassium phosphate buffer (pH 7.4) and 5 mM  $\text{MgCl}_2$ , final concentrations, at 37°C for 2 mins. The reactions were initiated by the addition of NADPH (1 mM, final concentration), incubated for 10 min, and reactions quenched by the addition of half the reaction volume of cold acetonitrile. The precipitated protein was removed by centrifugation and an aliquot of each sample was analyzed by HPLC with in-line radioactivity detection. For recombinant P450 enzymes, [ $^{14}$ C]midostaurin (10  $\mu$ M) was incubated with recombinant CYP450 (1 mg/mL for CYP1A1, CYP1A2, CYP2C8,

## DMD #72744

CYP2C9, CYP2C19, CYP2D6, CYP2E1, CYP3A5; 2.5 mg/mL for CYP2A6, CYP2B6) for 60 min.

**In vitro inhibition and induction of cytochrome P450 (CYP) enzymes:** The potential for reversible and time-dependent inhibition (TDI) of CYP enzyme activity by midostaurin, CGP52421, and CGP62221 was assessed using pooled human liver microsomes (HLM) (n= 50 donors, mixed gender, BD Biosciences, Bedford, MA). The enzyme activity was assessed using several probe substrates whose metabolism is known to be CYP enzyme-selective. For reversible inhibition, incubations were composed of (final concentrations): potassium phosphate buffer (100 mM, pH 7.4),  $\beta$ -NADPH (1 mM), magnesium chloride (5 mM), microsomal protein (0.025 – 0.5 mg/mL), probe substrate concentrations ( $\leq$  their  $K_m$  values), and test compound (0.5-100  $\mu$ M). After a 3-min preincubation, the reactions were initiated by addition of  $\beta$ -NADPH and terminated by addition of acetonitrile (2 volumes). Reactions were previously shown to be linear with respect to time and protein concentration (results not shown). For TDI, test compound was pre-incubated (37°C) with HLM. The pre-incubation contained (final concentrations): 100 mM potassium phosphate buffer (pH 7.4), 5 mM  $MgCl_2$ , 1 mM  $\beta$ -NADPH. The pre-incubations were initiated by addition of  $\beta$ -NADPH. After pre-incubation (0 – 30 min), aliquots were removed and transferred to an enzyme activity assay mixture (with 20-fold dilution) to determine activity remaining. The activity assay mixture consisted of (final concentrations): respective probe substrate, 1 mM  $\beta$ -NADPH, 5 mM  $MgCl_2$ , 100 mM potassium phosphate buffer (pH 7.4). The assay incubations were terminated by addition of acetonitrile. All probe substrate metabolism was assessed by LC-MS/MS analysis of specific metabolite formation. The potential for midostaurin,

## DMD #72744

CGP52421, and CGP62221 to act as inducers of CYP enzymes was evaluated in primary human hepatocytes of three individual donors using both mRNA quantification (real-time polymerase chain reaction) and CYP activity measurements (LC-MS/MS of selective CYP probe substrate metabolism, as stated above). Human hepatocytes were treated with midostaurin at a concentration range of 0-25  $\mu$ M, and CGP52421 and CGP62221 at a concentration range of 0-10  $\mu$ M for 48 h in addition to positive control inducers. Cell viability measurements after the treatment period found acceptable viability with midostaurin and its active metabolites and the positive control inducers.

**Pharmacokinetic Analyses:** The following pharmacokinetic parameters were determined by fitting the concentration-time profiles into a noncompartmental model with an iterative nonlinear regression program (WinNonlin software version 4.0, Pharsight, Mountain View, CA): area under the blood/plasma drug concentration-time curve between time 0 and time t ( $AUC_{0-t}$  or  $AUC_{last}$ ); AUC until time infinity ( $AUC_{0-\infty}$ ); highest observed blood/plasma drug concentration ( $C_{max}$ ); time to highest observed drug concentration ( $t_{max}$ ); apparent terminal half-life ( $t_{1/2}$ ); apparent volume of distribution of parent drug ( $V_z/F$ ) calculated as  $Dose/(AUC \cdot \lambda_z)$ , where F is the oral bioavailability and  $\lambda_z$  is the terminal rate constant; apparent steady-state volume of distribution of parent drug ( $V_{ss}/F$ ) calculated as  $(Dose) (AUMC)/(AUC)^2$ , where AUMC is the area under the first moment of the concentration-time curve; and the apparent oral clearance ( $CL/F$ ) was calculated as  $Dose/AUC_{0-\infty}$ .



## Results:

**Absorption:** In human, the absorption of midostaurin was rapid after oral administration in a diluted microemulsion, with the average peak plasma concentration of total radioactivity observed between 1-3 h post dosing. The extent of oral absorption can be estimated when radiolabeled drug is administered (Lin, et. al. 2012). Midostaurin oral absorption was estimated to be high since only 3.43% of unchanged midostaurin was found in the feces (Table 4) and midostaurin was confirmed to be stable in the *in vitro* fecal incubation study (Novartis data on file). Absorption can also be estimated from the radioactive dose recovered in the urine and the total radioactive dose recovered in the feces as oxidative metabolites. The mean radioactivity dose recovered in the urine was 4% and the mean radioactivity dose recovered in the feces in the forms of parent and metabolites were 3.43% (recovery normalized 4.8%) and 63.8% (recovery normalized 89.6%), respectively (Table 4). Based on the recovery normalized values 94.5% (a total of 67.2% in 144 h feces), the oral absorption in the microemulsion formulation was estimated to be high (>90%).

**Pharmacokinetics of Total Radioactivity, Midostaurin, Metabolite CGP52421 (epimers 1 and 2) and CGP62221 in Healthy Volunteers:** The mean plasma concentration-time profiles of total radioactivity, unchanged midostaurin, and pharmacologically active metabolites CGP52421 (epimers 1 and 2) and CGP62221 after a single oral administration of [ $^{14}\text{C}$ ] midostaurin after a dose of 50 mg are presented in Figure 2. The mean pharmacokinetic parameters of total radioactivity, unchanged midostaurin, CGP52421 (epimers 1 and 2) and CGP62221 were determined by noncompartmental analysis (Table 1).

## DMD #72744

The mean  $C_{\max}$  values for total circulating radioactivity, unchanged midostaurin, CGP52421 (epimers 1 and 2), and CGP62221 were 2160 ng-Eq/ml, 1240 ng/ml, 328 ng/ml, and 562 ng/ml and peaked at 2.0, 1.7, 3.3, and 3.2 hours, respectively (Table 1). The mean  $AUC_{(0-\infty)}$  values of total circulating radioactivity, unchanged midostaurin, CGP52421 (epimers 1 and 2), and CGP62221 were  $165 \times 10^3$  ng Eq•h/ml,  $15.7 \times 10^3$  ng•h/ml,  $146 \times 10^3$  ng•h/ml, and  $27.1 \times 10^3$  ng•h/ml, respectively (Table 1). The mean apparent terminal elimination half-lives of the total circulating radioactivity, unchanged midostaurin, CGP52421 (epimers 1 and 2), and CGP62221 were 134, 20.3, 495, and 33.4 h, respectively. The long terminal radioactivity elimination half-life was mainly attributed to CGP52421 (epimers 1 and 2), a major circulating metabolite with a plasma exposure ( $AUC_{0-\infty}$ ) approximately 9-fold higher than that of midostaurin. It was noticed that the last detectable time point varied from 48 to 2016 h for different components. Therefore, the individual component's AUC% to the total AUC could vary significantly based on which last time point was used for calculation. Using LC/MS/MS, the mean calculated apparent oral volume of distribution ( $V_z/F$ ) and clearance (CL) were 98.9 L, and 3.79 L/h, respectively (Table1).

**Excretion and Mass Balance in Urine and Feces:** After a single oral dose of 50 mg of [ $^{14}\text{C}$ ] midostaurin, the excretion of radioactivity from all six subjects in urine (for 7 days) and feces (for 20 days) is presented in Table 2. Over the seven days collection period, the percent recovery of total dose in urine ranged from 3.26 to 5.38% ( $4.00 \pm 0.73$ , mean  $\pm$  SD), whereas the percentage of dose in feces ranged from 66.8 to 77.9 % ( $72.7 \pm 4.59$ ). As the total radiolabeled dose recovered was less than 85% within the first 7 days, additional fecal samples were collected on days 8, 9, 13, 20, and 83. The excretion rate

## DMD #72744

calculated based on the total radioactivity data from fecal samples collected from days 9, 13, and 20 and was 0.73, suggesting that radioactivity recovered on each day is only 73% as compared to that from its previous day. Therefore, the estimated radioactivity recovered in feces for 20 days ranged from 71.6% to 84.0% (average  $77.6 \pm 4.72$ ), and the total radioactivity recovered ranged from 75.6 to 88.1% of dose (average  $81.6 \pm 4.85$ ). The radioactivity was detectable only in one subject on day 83. In summary, the radioactivity was excreted predominantly in the feces, averaging 77.6% of the total dose. Renal excretion was minor, accounting for 4.0% of the total dose. The radioactivity recovered on days 7 and 20 was 76.7% and 81.6%, respectively; indicating that majority of the radioactivity was excreted within the first week.

**Metabolite Profiling:** The metabolite profile summarizing the pharmacokinetics of midostaurin and its metabolites in plasma and percentage of midostaurin and its metabolites in excreta are presented in Table 3 and Table 4, respectively. A representative HPLC radio chromatogram of circulating metabolites is shown in Figure 3A. In plasma, major circulating components were unchanged midostaurin, P38.7 (CGP62221) and P39.8 (epimer 2 of CGP52421) accounting for 22% (midostaurin), 28% (P38.7) and 33% (P39.8) of the total plasma exposure ( $AUC_{0-96h}$ ), respectively. At early time points (up to 1 h) post-dose, the predominant radiolabeled plasma component was midostaurin, accounting for 67- 96% of the radio-chromatogram. At later time points (4-96 h), the predominant components were midostaurin, P38.7 and P39.8. Other major metabolites detected in plasma included P33 (*O*-desmethyl derivative of P39.8), P37.7 (epimer 1 of CGP52421) and P29.6B (*O*-desmethyl derivative of P37.7), accounting for 7.1%, 5.3% and 2.5%, of the total plasma exposure ( $AUC_{0-96h}$ ), respectively.

## DMD #72744

Representative HPLC radio-chromatograms for metabolites in urine and feces are shown in Figure 3B, and Figure 3C, respectively. Unchanged midostaurin was a minor component in the fecal profile, accounting for 3.43% of the dose, suggesting that metabolism is the major elimination mechanism for midostaurin in human. In addition to unchanged drug, a total of fifteen metabolites were detected in the feces. P29.6B (a combination of *O*-desmethyl and monohydroxyl), the major metabolite, accounted for 26.7% of the total administered dose. Other major metabolites included P27.9 (dihydroxy- midostaurin, 5.75% of the dose), P33.6 (monohydroxy- midostaurin, 4.94% of the dose), P28.8B (*O*-desmethyl derivative of monohydroxy- midostaurin, 4.83% of the dose), P33 (*O*-desmethyl and monohydroxy-midostaurin; 4.15% of the dose) and P38.7 (*O*-desmethyl midostaurin; 3.65% of the dose). No conjugated metabolites were detected in the feces. In the urine, P6B, the hippuric acid, derived by conjugation of glycine with benzoic acid metabolite of midostaurin, was the predominant metabolite. Trace amount of P6 (benzoic metabolite derived from amide hydrolysis) was also identified in urine. Together, P6 and P6B accounted for 2.6% of the dose. Unchanged midostaurin was not detected in urine.

**Metabolite Characterization by Mass Spectrometry:** Metabolite structures were characterized by LC/MS/MS using a combination of full and product ion scanning techniques and elemental composition by exact mass measurement. The structure of major metabolites, where possible, was supported by comparisons of their chromatographic retention times and mass spectral fragmentation patterns with those of synthetic standards.

## DMD #72744

Under positive ESI, midostaurin had a protonated ion at  $m/z$  571 with characteristic fragment ions observed at  $m/z$  436, 394, 362, 348, 260 and 192 (as illustrated in Figure 4). The formation of the above fragment ions was tentatively interpreted in Table 5. High resolution mass spectral information for each of these major fragment ions supported the proposed fragmentation. Analogous fragment ions were observed in the mass spectra of the metabolites, which allowed localization of metabolic changes to the pyrrolidinone, benzene rings of the staurosporinone moiety, or benzamide part of the molecule. This information, together with accurate mass data on  $[M + H]^+$  ions and fragments, and comparisons with available reference compounds (P6, P6B, P37.7, P38.7 and P39.8), allowed the assignment of the metabolite structures shown in Figure 5. Detailed characterization of midostaurin metabolites are shown in the Supplemental data section.

**Metabolite pathways of Midostaurin in human:** There appeared to be five primary metabolic reactions involved in the biotransformation of midostaurin in humans: (1) *O*-demethylation led to the formation of P38.7, accounting for elimination of 3.7% of the dose. *O*-demethylation followed or preceded by hydroxylation led to the formation of the metabolites P21.2, P22.6B, P28.8B, P29.6B and P33, which together accounted for elimination of 38.1% of the dose; (2) hydroxylation at the benzene moiety of the staurosporinone led to the formation of P33.6, P34.5 and P35.3, which accounted for elimination of 8.7% of the dose; (3) hydroxylation at the pyrrolidinone ring led to the formation of P37.7 and P39.8, which accounted for elimination of 2.9% of the dose. This metabolism pathway followed or was preceded by further hydroxylation, *O*-demethylation or *N*-demethylation led to formation of numerous metabolites, which

## DMD #72744

together accounted for elimination of more than 40% of the dose; (4) amide bond hydrolysis: hydrolysis of the amide bond led to the formation of P6, which underwent subsequent biotransformation reaction by conjugating with glycine to form hippuric acid (P6B). Together P6 and P6B accounted for elimination of 2.6% of the dose; (5) *N*-demethylation led to formation of P22.6, which was observed only in the plasma. *N*-demethylation coupled with hydroxylation or *O*-desmethylation led to the formation of P15.5 and P23.3, which were observed in the feces accounting for elimination of 2.6% of the dose.

### Protein binding in animals and humans

The *in vitro* plasma protein binding of midostaurin, CGP52421 and CGP62221 in the rat, dog and human was determined by equilibrium gel filtration. All three analytes were extensively bound to plasma proteins (>99.8%) in all species. Table 6 shows the mean plasma protein binding parameters for midostaurin and the metabolites respectively in rats, dogs and humans. In rats and dogs the protein binding of the three components was independent of concentration ( $f_u\%$  ranging from 0.08 to 0.239) over the tested concentration range of 100 - 47300 ng/mL. In humans, protein binding was concentration dependent with  $f_u\%$  of 0.01- 0.202 at a concentration of 100 - 43500 ng/mL. The  $f_u$  of midostaurin and its metabolites in humans at clinically relevant steady state concentration range did not appear to be concentration dependent ( $C_{max}$ : ~1200 – 5300 ng/mL at the dose of 50 mg b.i.d. in AML patients). At clinically relevant concentrations there was a species difference between rat and dog ( $f_u\%$ , 0.08-0.239) versus human ( $f_u\%$ , 0.01-0.0375) (Table 6).

### **Metabolism of Midostaurin by Human Liver Microsomes and Recombinant**

**Cytochrome P450s:** The formation of in vitro hepatic oxidative metabolism of midostaurin involved hydroxylation and demethylation was found to be predominantly catalyzed by CYP3A4. These primary metabolites were further metabolized by CYP3A4 to the metabolite(s) containing transformations both in recombinant CYP3A4 and in HLM test systems. The kinetic parameters  $K_m$  and  $V_{max}$  corresponding to CGP52421 and CGP62221 were 1.47  $\mu M$  and 2.86 pmol/min/pmol CYP3A4 and 0.506  $\mu M$  and 0.814 pmol/min/pmol CYP3A4, respectively for recombinant CYP3A4, and 2.19  $\mu M$  and 136 pmol/min/mg protein and 1.16  $\mu M$  and 47.3 pmol/min/mg protein, respectively for human liver microsomes.

### **In vitro inhibition and induction of cytochrome P450 (CYP) enzymes for Midostaurin and its two metabolites**

Midostaurin showed potent inhibition of CYP1A2, CYP2C8, CYP2C9, CYP2D6, CYP2E1 and CYP3A (IC<sub>50</sub> values between 0.5 and 5  $\mu M$ ). For other CYP activities (CYP2A6, CYP2B6, and CYP2C19), very little or no inhibition was observed up to 100  $\mu M$  midostaurin. CGP62221 and CGP52421 were both found to be relatively potent inhibitors of CYP3A activities with approximate IC<sub>50</sub> values of 1.0 and 2.0  $\mu M$ , respectively. CGP62221 also showed potent inhibition of CYP1A2, CYP2C8, CYP2C9 (IC<sub>50</sub> values <1-5.0  $\mu M$ ) whereas CGP52421 inhibited CYP2D6 activity with an approximate IC<sub>50</sub> value of 5.0  $\mu M$  and showed moderate inhibitory potency for CYP1A2, CYP2C8, and CYP2C9 (IC<sub>50</sub> values between 15 and 45  $\mu M$ ). No time-dependent inhibition of CYP1A2, CYP2B6, CYP2C9, CYP2C19, or CYP2D6 was observed at concentrations up to 50  $\mu M$  for midostaurin, CGP62221, or CGP52421. Time-dependent

## DMD #72744

inhibition of CYP3A by midostaurin, CGP52421, and CGP62221 was observed. Very weak time-dependent inhibition of CYP2C8 by midostaurin was also observed.

Midostaurin, CGP52421 and CGP62221 induced mRNA levels of CYP1A1, CYP1A2, CYP2B6, CYP2C8, CYP2C9, CYP2J2, CYP3A4, CYP3A5, UGT1A1 and MRP2. CYP1A2, CYP2B6, CYP2C8, CYP2C9 and CYP2C19 activities were also induced by midostaurin and its metabolites.



## Discussion

Midostaurin pharmacokinetics, mass balance, absorption, metabolism and excretion were determined in healthy volunteers to support drug development and regulatory filings. The results are summarized as a quantitative mass balance diagram (Shepard, 2015) in Figure 6. [ $^{14}\text{C}$ ] midostaurin was well tolerated after a single oral 50 mg dose formulated as a microemulsion, as no adverse events were reported during the study. Midostaurin oral absorption is high (>90%) as only 3.43% of intact drug was found in the feces (Table 4), which was likely unabsorbed drug as midostaurin is stable in the gastrointestinal milieu. Preclinical studies also showed high absorption in rats (>90%) (Supplemental data) and the rat is a predictive and commonly used model of absorption in humans (Chiou and Barve, 1998; Lin, et al. 2012). As midostaurin is a lipophilic drug (cLogP >5) with low aqueous solubility (<0.001 mg/mL) and high absorption, midostaurin can be classified as a BCS class II (Amidon et al. 1995) drug in human, indicating that absorption and systemic exposure can be dose or formulation dependent. Here the solubilizing microemulsion formulation was used to maximize midostaurin absorption. The exposures of midostaurin in the microemulsion formulation reported in this human ADME study were similar to those observed with a 50 mg microemulsion capsule formulation (Wang et al., 2008).

Midostaurin exact absolute human oral bioavailability could not be estimated with high confidence, due to lack of intravenous data. In rat and dog, the bioavailability was low to moderate ranging from 9.3-48.5% (Supplemental data). Using the average preclinical bioavailability method (Vuppugalla et al., 2011), midostaurin's human oral bioavailability could be crudely estimated to be low to moderate, ~ 30%, based on rat and

DMD #72744

dog (Supplemental data). As absorption was >90%, this suggested a high first-pass metabolism in the gut in addition to liver first pass, consistent with findings in the rat which had a high first pass metabolism in gut (90% absorption and 9% bioavailability).

In plasma, midostaurin and its major two metabolites were analyzed with LC/MS/MS (Table 1) and radio-detection (Table 3). With radio-detection, the majority of the total circulating radioactivity based on 96 h data was mainly comprised of metabolites, as the exposure ( $AUC_{0-96}$ ) of unchanged midostaurin accounted for only 22.0% of the total exposure (Table 3). The major circulating metabolites determined were CGP52421 (7-hydroxylated midostaurin, epimer 2), CGP62221 (*O*-desmethyl-midostaurin) accounting for 32.7 and 27.7% of exposure, respectively. Pharmacokinetic analyses suggested that the absorption was relatively rapid as indicated by a  $T_{max}$  of ~1-3 h with both detection methods.

Due to radio-detection limitations, LC/MS/MS was also used to quantify midostaurin, CGP52421 (total exposure measured; epimer 1 and 2 not separated) and CGP62221 up to 83 day (Table 1). Based on  $AUC_{0-last}$ , CGP52421 exposure was 9-fold higher than midostaurin. In contrast, CGP62221 exposure was similar to midostaurin. The mean apparent oral plasma clearance ( $CL/F$ ) of midostaurin was low at 3.79 L/h compared to the human hepatic blood flow (87 L/h). The mean apparent oral volume of distribution ( $V_z/F$ ) of midostaurin was 98.9 L, higher than the total body water (42 L), indicating tissue distribution (Table 1). The terminal half-life of midostaurin was long (20.3 h) and similar to that of CGP62221 (33.4 h) but much shorter than that of CGP52421 (495 h) (Table 1). Based on the in vitro data from the HLM and recombinant CYPs, midostaurin was mainly metabolized by CYP3A4 to form CGP62221 and CGP52421 (Supplemental

## DMD #72744

data). These two primary metabolites were further metabolized by CYP3A4 to the metabolite(s) containing both hydroxylation and demethylation transformations, which made it difficult to accurately estimate the kinetic parameters associated with each of the primary metabolic reactions. Nevertheless, the hydroxylation and demethylation reactions showed similar catalytic efficiencies.

In human plasma the major primary metabolite P39.8 (epimer 2 of CGP52421) was detected in both preclinical species while the primary metabolite P38.7 (CGP62221) was only found in dog, but not in rat (Supplemental data). Secondary metabolites derived from *O*-demethylation and hydroxylation (P29.6B and P33) were also detected (2.5% of AUC; P29.6B and 7.1% of AUC; P33). Based on the chromatographic elution order, P29.6B and P33 were proposed as the CGP52421 epimer 1 and epimer 2 derivatives of P38.7, respectively.

Renal excretion was a minor elimination route for midostaurin in human, with P6B, a hippuric acid metabolite, being detected as the main component. Hippuric acids are normal constituents in urine of mammals, and are readily excreted in urine via the organic anion transport system. Analysis of control human samples showed that hippuric acid was excreted in urine as an endogenous product, albeit at a very low level. Midostaurin was not detectable in urine.

In feces, the major metabolite was P29.6B (26.7% of the dose) (Table 4). Minor metabolites that were detected included: P33 (4.15% of dose), P37.7 (2.85% of dose), P38.7 (3.65% of dose), and P39.8 (trace amount) (Table 4). While P39.8 (epimer 2 of CGP52421, 32.7%) predominated in the plasma, only traces were detected in the feces. In comparison, P37.7 (epimer 1 of CGP52421) had low levels in both plasma

DMD #72744

(5.27%) and feces (2.85%) (Table 3 and Table 4). Possibly, once P37.7 and P39.8 were formed in the liver, P37.7 appeared to be further metabolized much faster than P39.8 forming P29.6B (combination of epimer 1 and CGP62221) which was subsequently detected in feces as the major metabolite.

In AML patients, total midostaurin exposures were overall significantly higher than those in preclinical species as the human clearance (estimated to be 0.016 L/h/kg based on CL/F 0.05 L/h/kg and F 30%) is much lower than that in animals (0.98 and 0.9 L/h/kg in rats and dogs, respectively). The total exposure multiples (animal/human) from rats and dogs (general toxicology species) relative to AML patient exposures at steady state (50 mg bid) were less than 1, e.g. 0.06-0.09 for midostaurin, 0.03-0.06 for CGP52421 (total measured) and 0.02 for CGP62221 (dog only). When correcting for protein binding species differences with lower  $f_u$  in human (Table 6), the free exposure multiples were improved by 5-10 fold, e.g. 0.3-0.7 for midostaurin, 0.3-0.68 for CGP52421 and 0.11 for CGP62221 (dog only). While the free exposure multiples appeared more favorable, after considering potential assay limitations due to very high protein binding, it was decided to report both total and free concentrations for safety margin calculations to health authorities.

*In vitro* efficacy studies using transfected cell systems were conducted. The metabolites were shown to inhibit FLT3-ITD dependent cell proliferation with  $IC_{50}$  values of 656 nM (367 ng/mL) (CGP52421) and 28 nM (15.6 ng/mL) (CGP62221) compared to 39 nM (22 ng/mL) for midostaurin (data on file). Midostaurin showed similar pharmacological activity to CGP62221 and was 10 fold higher than CGP52421. Both CGP52421 epimers showed similar *in vitro* pharmacological activities. The high systemic exposures of

## DMD #72744

metabolites CGP52421 and CGP62221 in humans, along with their relatively potent cell-based  $IC_{50}$  for FLT3-ITD inhibition, suggested that the antileukemic activity in AML patients may also be maintained by metabolites (Zarrinkar et al, 2009). To evaluate pharmacodynamics contributions, the total exposure of the three components instead of midostaurin alone was linked to efficacy in clinical studies.

Most drugs with long radioactivity half-lives show lower recovery (Roffey et al. 2011) in part due to suboptimal sampling and relatively short collection times. In this study, an innovative mass balance approach which calculated excretion rates using days 8, 9, 13 and 20 was introduced. Through careful mass-balance study design, the total recovery achieved in excreta was good (81.6%) (Table 2, Table 4, Figure 6).

Concomitant medications, e.g. CYP3A modulators, may impact pharmacokinetics of midostaurin (Dutreix et al., 2013). A high fraction of drug metabolized by CYP3A4 ( $fm_{CYP3A}$ ) of over 0.9 was confirmed in a clinical DDI study, where midostaurin exposure increased over 6 – 10 fold with ketoconazole (CYP3A4 inhibitor). The  $fm_{CYP3A}$  was also verified using PBPK modeling (Data on file).

Midostaurin and its metabolites showed both reversible inhibition and induction for some CYP enzymes. Midostaurin and its metabolites also showed time-dependent inhibition of CYP3A *in vitro*. Induction of CYP3A mRNA with little change in its enzyme activity was consistent with the time-dependent inhibition properties of midostaurin, CGP52421 and CGP62221 toward CYP3A. Midostaurin and its active metabolites, CGP52421 and CGP62221, may cause changes in exposure of co-administered compounds primarily cleared by the CYP3A enzyme. For other CYP enzymes, the interplay of inhibition and

## DMD #72744

induction may need to be considered, and it would be challenging to assess the net effects of potential DDI.

Overall, midostaurin is a BCS/BDDCS class II drug in human (Benet 2011, Custodio et. al., 2008) given its low aqueous solubility (<0.001 mg/mL), high absorption (>90%), high log P along with extensive metabolism (> 90%). This is consistent with rat BDDCS, i.e. high absorption (>90%) and extensive metabolism (>90%) (Supplemental Data). The major circulating components were midostaurin, CGP52421 and CGP62221. As midostaurin, CGP52421 and CGP62221 are metabolized mainly by CYP3A4 and are inhibitors/inducers for CYP3A, potential drug-drug interactions with mainly CYP3A4 modulators/substrates could be expected.

### **Acknowledgements**

The authors would like to thank Dr. Tapan Ray and Grazyna Ciszewska for providing the radiolabeled drug substance, Sebastien Balez for supporting bioanalytical work, Drs. Tao Zhang and Rakesh Gollen for assistance with early data compilation, Drs. Heidi Einolf and Imad Hanna for help with DDI in vitro data, Drs. Mark Kagan and Jim Mangold for helpful metabolism discussions. The clinical phase of this study was conducted under the supervision of Margaret Woo (Novartis) and James C. Kisicki, M.D., MDS Pharma Services, Lincoln, NE, USA.

DMD #72744

### **Authorship Contributions**

Participated in research design: He, Tran, Gu

Conducted experiments: Zhang, Tedesco, Tran, Gu, Klein, Gatlik

Contributed new reagents or analytic tools: Tran, He

Performed data analysis: Heimbach, Tran, He, Lin, Gu, Klein, Gatlik

Wrote or contributed to the writing of the manuscript: He, Heimbach, Lin, Tran, Gu

## References

- Amidon GL, Lennernäs H, Shah VP, Crison JR (1995) A theoretical basis for a biopharmaceutic drug classification: the correlation of in vitro drug product dissolution and in vivo bioavailability. *Pharm Res*. **12**: 413–20.
- Benet LZ, Broccatelli F and Oprea TI (2011) BDDCS Applied to Over 900 Drugs. *AAPS J*, **13**: 519–547.
- Birg F, Courcoul M, Rosnet O, Bardin F, Pebusque MJ, Marchetto S, Tabilio A, Mannoni P, and Birnbaum D (1992) Expression of the FMS/KIT-like gene FLT3 in human acute leukemias of the myeloid and lymphoid lineages. *Blood* **80**:2584-2593.
- Breitenbuecher F, Markova B, Kasper S, Carius B, Stauder T, Böhmer FD, Masson K, Rönstrand L, Huber C, Kindler T and Fischer T (2009) A novel molecular mechanism of primary resistance to FLT3-kinase inhibitors in AML. *Blood* **113**:4063-4073
- Chiou WL and Barve A (1998) Linear correlation of the fraction of oral dose absorbed of 64 drugs between humans and rats. *Pharm Res* **15**:1792-1795.
- Dutreix C, Munarini F, Lorenzo S, Roesel J, and Wang Y (2013) Investigation into CYP3A4-mediated drug-drug interactions on midostaurin in healthy volunteers. *Cancer Chemotherapy & Pharmacology* **72**:1223.
- Fabbro D, Ruetz S, Bodis S, Pruschy M, Csermak K, Man A, Campochiaro P, Wood J, O'Reilly T, and Meyer T (2000) PKC412--a protein kinase inhibitor with a broad therapeutic potential. *Anticancer Drug Des* **15**:17-28.
- Fischer T, Stone RM, DeAngelo DJ, Galinsky I, Estey E, Lanza C, Fox E, Ehninger G, Feldman EJ, Schiller GJ, Klimek VM, Nimer SD, Gilliland DG, Dutreix C, Huntsman-Labed A, Virkus J, and Giles FJ (2010) Phase IIB trial of oral midostaurin (PKC412), the FMS-like tyrosine kinase 3 receptor (FLT3) and multi-targeted kinase inhibitor, in patients with acute myeloid leukemia and high-risk myelodysplastic syndrome with either wild-type or mutated FLT3. *J Clin Onc* **28**:4339-4345.
- Furukawa Y, Vu H A, Akutsu M, Odgerel T, Izumi T, Tsunoda S, Matsuo Y, Kirito K, Sato Y, Mano H and Kano Y (2007) Divergent cytotoxic effects of PKC412 in combination with conventional antileukemic agents in FLT3 mutation-positive versus -negative leukemia cell lines. *Leukemia* **21**:1005–1014
- Hatcher JM, Weisberg E, Sim T, Stone RM, Liu S, Griffin JD, and Gray NS (2016) Discovery of a Highly Potent and Selective Indenoindolone Type 1 Pan-FLT3 Inhibitor. *ACS Med Chem Lett* **7**:476–481
- Kiyoi H, Naoe T, Nakano Y, Yokota S, Minami S, Miyawaki S, Asou N, Kuriyama K, Jinnai I, Shimazaki C, Akiyama H, Saito K, Oh H, Motoji T, Omoto E, Saito H, Ohno R, and Ueda R (1999) Prognostic implication of FLT3 and N-RAS gene mutations in acute myeloid leukemia. *Blood* **93**:3074-3080.
- Kottaridis PD, Gale RE, Frew ME, Harrison G, Langabeer SE, Belton AA, Walker H, Wheatley K, Bowen DT, Burnett AK, Goldstone AH, and Linch DC (2001) The presence of a FLT3 internal tandem duplication in patients with acute myeloid leukemia (AML) adds important prognostic information to cytogenetic risk group and response to the first cycle of chemotherapy: analysis of 854 patients from the



- United Kingdom Medical Research Council AML 10 and 12 trials. *Blood* **98**:1752-1759.
- Lin T, Heimbach T, Gollen R, and He H (2012) Mass Balance Studies in Animals and Humans *Encyclopedia of Drug Metabolism and Interactions* **III**:1–39. Available from: <http://onlinelibrary.wiley.com/doi/10.1002/9780470921920.edm029/pdf>. [last accessed 3 Jan 2017]
- Lowenberg B, Downing JR, and Burnett A (1999) Acute myeloid leukemia *N Engl J Med* **341**:1051-1062.
- Novartis Press Release (2016) Novartis drug PKC412 (midostaurin) receives Breakthrough Therapy designation from the FDA for newly-diagnosed FLT3-mutated acute myeloid leukemia (AML).
- Penner N, Xu L, and Prakash C (2012) Radiolabeled absorption, distribution, metabolism, and excretion studies in drug development: why, when, and how? *Chem Res Toxicol* **25**:513-531.
- Roffey SJ, Obach RS, Gedge JI and Smith DA What is the objective of the mass balance study? A retrospective analysis of data in animal and human excretion studies employing radiolabeled drugs (2007) *Drug Metab Rev* **39**(1):17-43.
- Rosnet O, Marchetto S, deLapeyriere O, and Birnbaum D (1991) Murine Flt3, a gene encoding a novel tyrosine kinase receptor of the PDGFR/CSF1R family. *Oncogene* **6**:1641-1650.
- Shepard T, Scott G, Cole S, Nordmark A, and Bouzom, F (2015) Physiologically Based Models in Regulatory Submissions: Output from the ABPI/MHRA Forum on Physiologically Based Modeling and Simulation. *CPT Pharmacometrics Syst Pharmacol* **4**: 221–225.
- Stone RM (2016) The Multi-Kinase Inhibitor Midostaurin (M) Prolongs Survival Compared with Placebo (P) in Combination with Daunorubicin (D)/Cytarabine (C) Induction (ind), High-Dose C Consolidation (consol), and As Maintenance (maint) Therapy in Newly Diagnosed Acute Myeloid Leukemia (AML) Patients (pts) Age 18-60 with FLT3 Mutations (mut): An International Prospective Randomized (rand) P-Controlled Double-Blind Trial (CALGB 10603/RATIFY [Alliance]). Presented at the 57th Annual Meeting of the American Society of Hematology. .
- Thiede C, Steudel C, Mohr B, Schaich M, Schakel U, Platzbecker U, Wermke M, Bornhauser M, Ritter M, Neubauer A, Ehninger G, and Illmer T (2002) Analysis of FLT3-activating mutations in 979 patients with acute myelogenous leukemia: association with FAB subtypes and identification of subgroups with poor prognosis. *Blood* **99**:4326-4335.
- Udayakumar N, Rajendiran C, Muthuselvan R (2006) A typical presentation of acute myeloid leukemia *J. Cancer Res Ther* **2**: 82-84
- Vuppugalla R, Marathe P, He H, Jones RDO, Yates JWT, Jones HM, Gibson CR, Chien JY, Ring BJ, Adkison KK, Ku MS, Fischer V, Dutta S, Sinha VK, Bjoernsson T, Lave T, and Poulin P (2011) PhRMA CPCDC initiative on predictive models of human pharmacokinetics, Part 4: Prediction of plasma concentration-time profiles in human from in vivo preclinical data by using the Wajima approach. *J Pharm Sci* **100**:4111-4126.

DMD #72744

- Wang Y, Yin OQ, Graf P, Kisicki JC, and Schran H (2008) Dose-and time-dependent pharmacokinetics of midostaurin in patients with diabetes mellitus. *J Clin Pharmacol* **48**:763-775.
- Weisberg E, Boulton C, Kelly LM, Manley P, Fabbro D, Meyer T, Gilliland DG, and Griffin JD (2002) Inhibition of mutant FLT3 receptors in leukemia cells by the small molecule tyrosine kinase inhibitor PKC412. *Cancer Cell* **1**:433-443.
- Weiss M and Gatlik E (2014) Equilibrium Gel Filtration to Measure Plasma Protein Binding of Very Highly Bound Drugs. *J Pharm Sci* **103**:752–759.
- Yanada M, Matsuo K, Suzuki T, Kiyoi H, and Naoe T (2005) Prognostic significance of FLT3 internal tandem duplication and tyrosine kinase domain mutations for acute myeloid leukemia: a meta-analysis. *Leukemia* **19**:1345-1349.
- Zarrinkar PP, Gunawardane RN, Cramer MD, Gardner MF, Brigham D, Belli B, Karaman MW, Pratz KW, Pallares G, Chao Q, Sprankle KG, Patel HK, Levis M, Armstrong RC, James J, Bhagwat SS (2009) AC220 is a uniquely potent and selective inhibitor of FLT3 for the treatment of acute myeloid leukemia (AML). *Blood* **114**(14):2984-92.

## Legends

Figure 1. Chemical structure of [ $^{14}\text{C}$ ] Midostaurin and related compounds

Figure 2. Plasma concentrations of radioactivity (inverted triangles), Midostaurin (circles), CGP52421 (squares) and CGP62221 (triangles) after a single 50 mg oral dose of [ $^{14}\text{C}$ ] Midostaurin.

Figure 3. Representative radio-chromatograms of Midostaurin in plasma 24h post dose (A), urine 0-72 h (B), and feces 0-144 h (C) after a single oral dose of [ $^{14}\text{C}$ ] Midostaurin to humans. Note that P6, P6B, P37.7, P38.7 and P39.8 were identified by retention times and CID product ion spectra that were similar to those of their synthetic standards, whereas the other metabolite structures were tentatively assigned as described under *Results*.

Figure 4. Product ion mass spectrum of Midostaurin

Figure 5. Metabolism of Midostaurin in human

Figure 6. Midostaurin quantitative mass balance diagram after oral dosing in human. Percentage values reflect values from after 144h, corrected for a recovery of 71.1%. After 20 days the recovery was 81.6%.

DMD #72744

TABLE 1

*Plasma pharmacokinetic parameters of midostaurin and metabolites after a single 50-mg oral dose of [<sup>14</sup>C] Midostaurin (mean ± SD, n=6) using LC/MS/MS up to 83 days*

Pharmacokinetic parameters <sup>a</sup>	Midostaurin <sup>a</sup>	CGP52421 (epimers 1 and 2) <sup>a</sup>	CGP62221 <sup>a</sup>	Total Radioactivity <sup>b</sup>
$C_{\max}$ (ng/mL) or (ngEq/mL)	1210 ± 360	328 ± 56.9	562 ± 71.2	2160 ± 383
$t_{\max}$ (h)	1.7 ± 1.0	3.3 ± 1.5	3.2 ± 0.8	2.0 ± 1.3
$T_{\text{last}}$ (h)	Range: 48-144 (median 108)	Range: 864 - 2016 (median 1344)	Range: 96 - 252 (median 168)	168
$AUC_{\text{last}}$ (ngh/mL) or (ngEq•h/mL)	15200 ± 5770	123000 ± 51700	26300 ± 8470	105000 ± 20800
$AUC_{0-\infty}$ (ngh/mL) or (ngEq•h/mL)	15700 ± 5900	146000 ± 59300	27100 ± 8880	165000 ± 27600
Apparent $t_{1/2}$ (h)	20.3 ± 6.7	495 ± 134	33.4 ± 10.2	134 ± 27.5
CL/F (L/h)	3.79 ± 2.09			
Predicted CL (L/h/kg) <sup>c</sup>	0.016 (Est. F=30%)			
Vz/F (L)	98.9 ± 31.2			
Predicted Vz (L/kg) <sup>d</sup>	0.42 (Est. F=30%)			

<sup>a</sup> Midostaurin, CGP52421 (epimers 1 and 2), and CGP62221 concentrations were determined using validated LC/MS/MS methods.

<sup>b</sup> Total radioactivity was determined by liquid scintillation counting.

<sup>c</sup> CL (L/h/kg) for rat and dog is 0.98 and 0.90, respectively (Supplemental data)

<sup>d</sup> Vss (L/kg) for rat and dog is 1.2 and 3.77, respectively (Supplemental data).

DMD #72744

TABLE 2

*Cumulative excretion of [ $^{14}\text{C}$ ] radioactivity in urine and feces after a single oral dose of 50 mg [ $^{14}\text{C}$ ]Midostaurin in humans (mean  $\pm$  SD, n=6)*

Time period (h)	Feces (% of dose)	Urine (% of dose)	Total (% of dose)
0-24	1.94 $\pm$ 1.34	1.68 $\pm$ 0.49	
0-48	13.81 $\pm$ 12.59	2.65 $\pm$ 0.64	
0-72	36.44 $\pm$ 13.50	3.45 $\pm$ 0.78	
0-168	72.7 $\pm$ 4.59	4.00 $\pm$ 0.73	
0-480	77.6 $\pm$ 4.72	-	81.6 $\pm$ 4.85
- Not measured			

DMD #72744

TABLE 3

*Pharmacokinetic parameters of Midostaurin and its metabolites in plasma after a single*

*50-mg oral dose of [<sup>14</sup>C]Midostaurin using radio-detection up to 96h (mean ± SD, n=6)*

Pharmacokinetic parameters <sup>a</sup>	P33 <sup>b</sup>	P37.7; CGP52421 epimer 1 <sup>b</sup>	P39.8; CGP52421 epimer 2 <sup>b</sup>	P38.7; CGP62221 <sup>b</sup>	Midostaurin <sup>b</sup>
C <sub>max</sub> (ngEq/ml)	69.9 ± 14.4	94.3 ± 16.6	327 ± 43.2	524 ± 76.9	1330 ± 424
t <sub>max</sub> (h)	44 ± 18	4.7 ± 1.6	6.7 ± 2.1	4.0 ± 0	1.9 ± 1.6
AUC <sub>0-96h</sub> (ngEq•h/ml)	5590 ± 1090	4120 ± 1000	25800 ± 2910	22500 ± 5870	18000 ± 6200
AUC <sub>0-96h</sub> (%)	7.12 ± 1.51	5.27 ± 1.45	32.7 ± 5.13	27.7 ± 2.66	22.0 ± 4.86

Major circulating metabolites are shown; other circulating metabolites were quantified and accounted for 5.32% AUC (P15.5: 0.77%, P22.6: 0.95% P23.3: 1.10%, P29.6B: 2.50%).

<sup>a</sup> Abbreviation definitions for PK parameters are denoted in the Pharmacokinetic Analysis in the Materials and Methods section.

<sup>b</sup> Midostaurin and its metabolites were determined by HPLC with radio-detection.

DMD #72744

TABLE 4

*Amount of Midostaurin and metabolites in urine (0-72h) and feces (0-144h) following a single oral dose of 50 mg [ $^{14}\text{C}$ ] Midostaurin (mean  $\pm$  SD; n=6)*

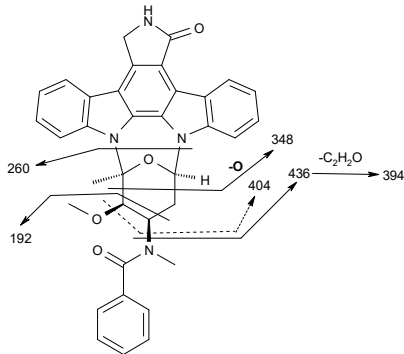
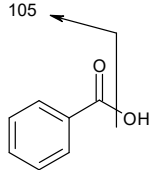
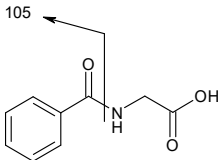
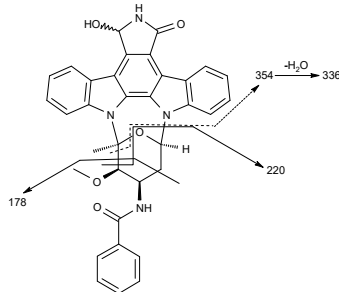
Feces	Feces (% of dose) [recovery corrected]
P15.5	1.67 $\pm$ 0.50
P21.2	1.64 $\pm$ 0.34
P22.6B	0.78 $\pm$ 0.28
P23.3	0.95 $\pm$ 0.29
P25.5	2.17 $\pm$ 0.81
P27.9	5.75 $\pm$ 0.97
P28.8B	4.83 $\pm$ 1.61
P29.6B	26.7 $\pm$ 4.04 [37.5]
P33	4.15 $\pm$ 0.53
P33.6	4.94 $\pm$ 0.49
P34.5	1.34 $\pm$ 0.46
P35.3	2.44 $\pm$ 0.96
P37.7; CGP52421 epimer 1	2.85 $\pm$ 0.45 [4.0]
P38.7; CGP62221	3.65 $\pm$ 0.61 [5.2]
P39.8; CGP52421 epimer 2	- <sup>a</sup>
Midostaurin	3.43 $\pm$ 1.63 [4.8]
<hr/>	
Feces	
Sum of metabolites (feces, 144h)	63.8 [89.6]
Total radioactivity (feces, 144h)	67.2 [94.5]
Total radioactivity (feces, 20 days)	77.6
<hr/>	
Urine	Urine (% of dose)
P6, P6B (urine, 72h)	2.62 $\pm$ 0.73
Midostaurin (urine, 72h)	0
Total radioactivity (urine, 144h)	3.9 [5.4]
<hr/>	
Excreta	(% of dose)
Sum of metabolites (excreta, 144h)	67.7 <sup>b</sup> [95.2]
Total radioactivity (excreta, 144h)	71.1 [100]
Fraction of Dose metabolized (excreta, 144h)	95.2
Total radioactivity (excreta 20 days)	81.6

<sup>a</sup> Trace amount detected, not quantifiable. <sup>b</sup> 95% metabolized after recovery correction using a factor of 1.4 or 100/71.1. Fraction of dose metabolized after recovery correction was >90% in both rats and dogs after an i.v. dose (Supplement data). This correction assumes that the disposition of the unrecovered radioactivity was similar to that of the recovered activity.

DMD #72744

TABLE 5

*Characteristic and proposed structures of Midostaurin metabolites*

Metabolite	[M+H] <sup>+</sup>	Fragment ions	Assigned structure
Midostaurin	571	192, 260, 348, 394, 404, 436	
P6	123	105, 79 (-CO <sub>2</sub> )	
P6B	180	162 (-H <sub>2</sub> O), 105	
P15.5	573	354, 336, 220, 178	

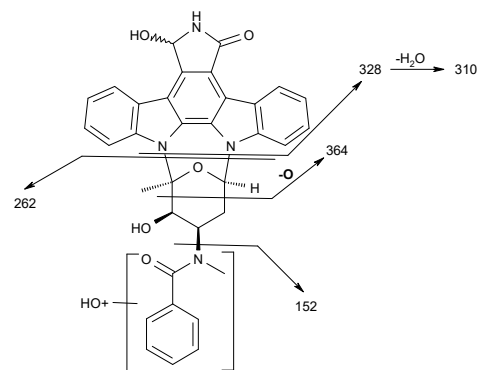


# DMD #72744

**P21.2**

589

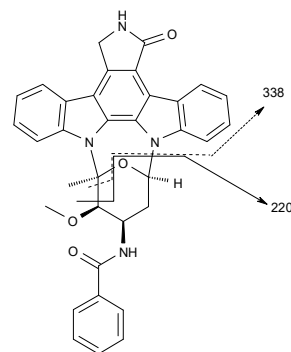
571 (-H<sub>2</sub>O), 364, 328,  
310, 262, 152



**P22.6**

557

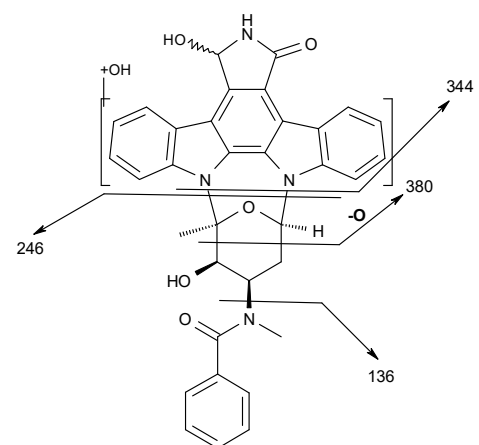
338, 220



**P22.6B**

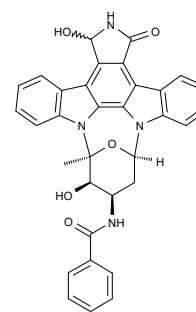
589

571 (-H<sub>2</sub>O), 380, 344,  
246, 136



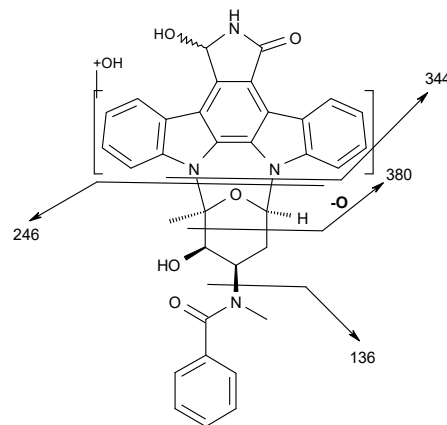
**P23.3**

559

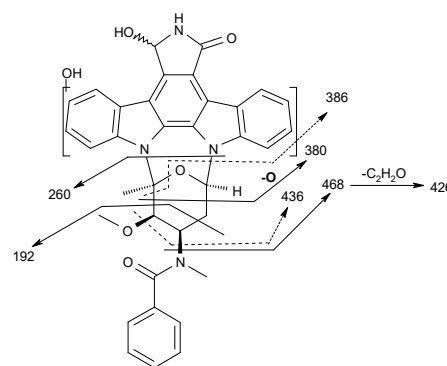


# DMD #72744

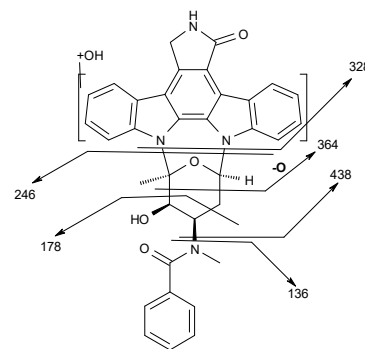
**P25.5** 589 571 (-H<sub>2</sub>O), 380, 344,  
246, 136



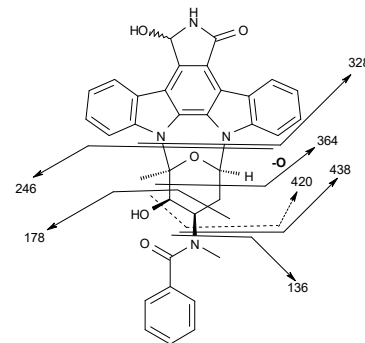
**P27.9** 603 585 (-H<sub>2</sub>O), 468, 436,  
426, 386, 380, 260,  
192



**P28.8B** 573 438, 364, 246, 178,  
136

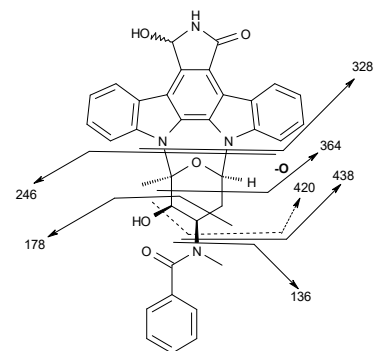


**P29.6B** 573 555 (-H<sub>2</sub>O), 438, 420,  
364, 328, 246, 178,  
136

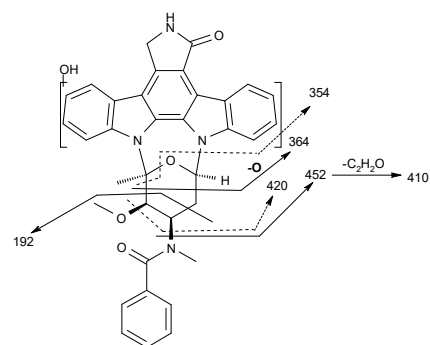


DMD #72744

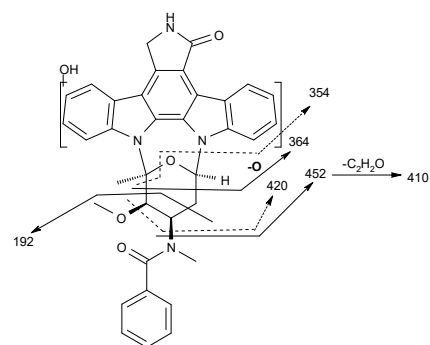
**P33** 573 555 (-H<sub>2</sub>O), 438, 420,  
364, 328, 246, 178,  
136



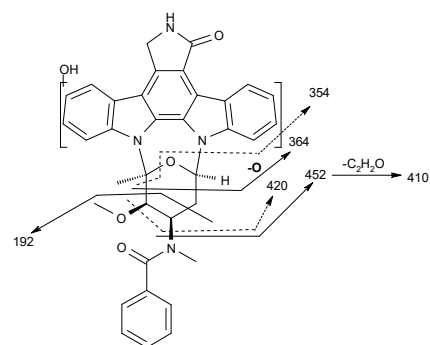
**P33.6** 587 452, 420, 410, 364,  
354, 192



**P34.5** 587 452, 420, 410, 364,  
354, 192

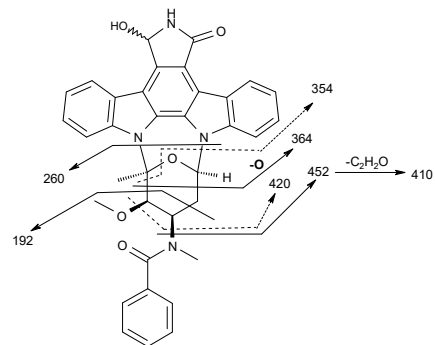


**P35.3** 587 452, 420, 410, 364,  
354, 192

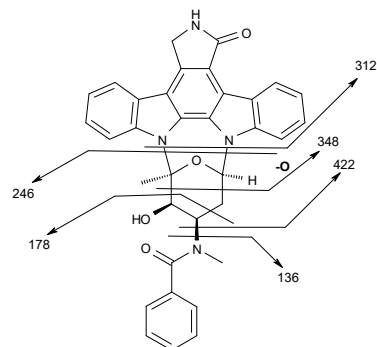


DMD #72744

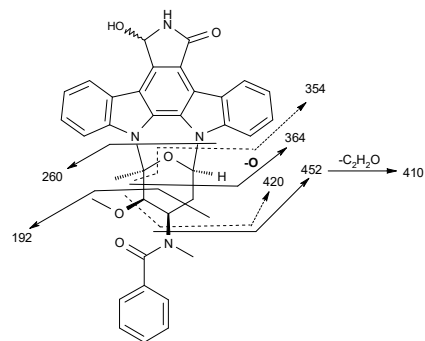
**P37.7** 587 569 (-H<sub>2</sub>O), 452, 420,  
(epimer 1 of 410, 364, 354, 260,  
CGP52421) 192



**P38.7** 557 422, 348, 312, 246,  
(CGP62221) 178, 136



**P39.8** 587 569 (-H<sub>2</sub>O), 452, 420,  
(epimer 2 of 410, 364, 354, 260,  
CGP52421) 192



DMD #72744

TABLE 6

Summary of mean plasma protein binding for midostaurin, CGP52421 and CGP62221 in rat, dog and human

	Concentration (ng/mL)	Rat, fraction unbound (%)	Dog, fraction unbound (%)	Human, fraction unbound (%)
<b>midostaurin</b>	<b>100-20,000</b>	<b>0.1 ± 0.02**</b>	<b>0.08 ± 0.01**</b>	
<b>midostaurin</b>	<b>100-10,000</b>			<b>0.01 - 0.02</b>
midostaurin	20,000			0.07
<b>CGP52421 (epimers 1 and 2)</b>	<b>141-39700</b>	<b>0.239 ± 0.0351**</b>		
<b>CGP52421 (epimers 1 and 2)</b>	<b>319-45200</b>		<b>0.204 ± 0.0454**</b>	
<b>CGP52421 (epimers 1 and 2)</b>	<b>1970-7790</b>			<b>0.0214 ± 0.0140</b>
CGP52421 (epimers 1 and 2)	13700-17000			0.155 ± 0.0332
CGP52421 (epimers 1 and 2)	29000-34600			0.202 ± 0.0412
CGP52421 (epimers 1 and 2)	overall: 1970 - 34600			range: 0.0214 - 0.202
<b>CGP62221</b>	<b>860-27200</b>	<b>0.227 ± 0.0907**</b>		
<b>CGP62221</b>	<b>925 - 47300</b>		<b>0.193 ± 0.0140**</b>	
<b>CGP62221</b>	<b>5470-6110</b>			<b>0.0375 ± 0.00605</b>
CGP62221	10100-11400			0.0976 ± 0.00252
CGP62221	39400-43500			0.198 ± 0.0140

\*Bold font denotes the values at clinically relevant concentration ranges

\*\*protein binding species difference compared to human

Figure 1

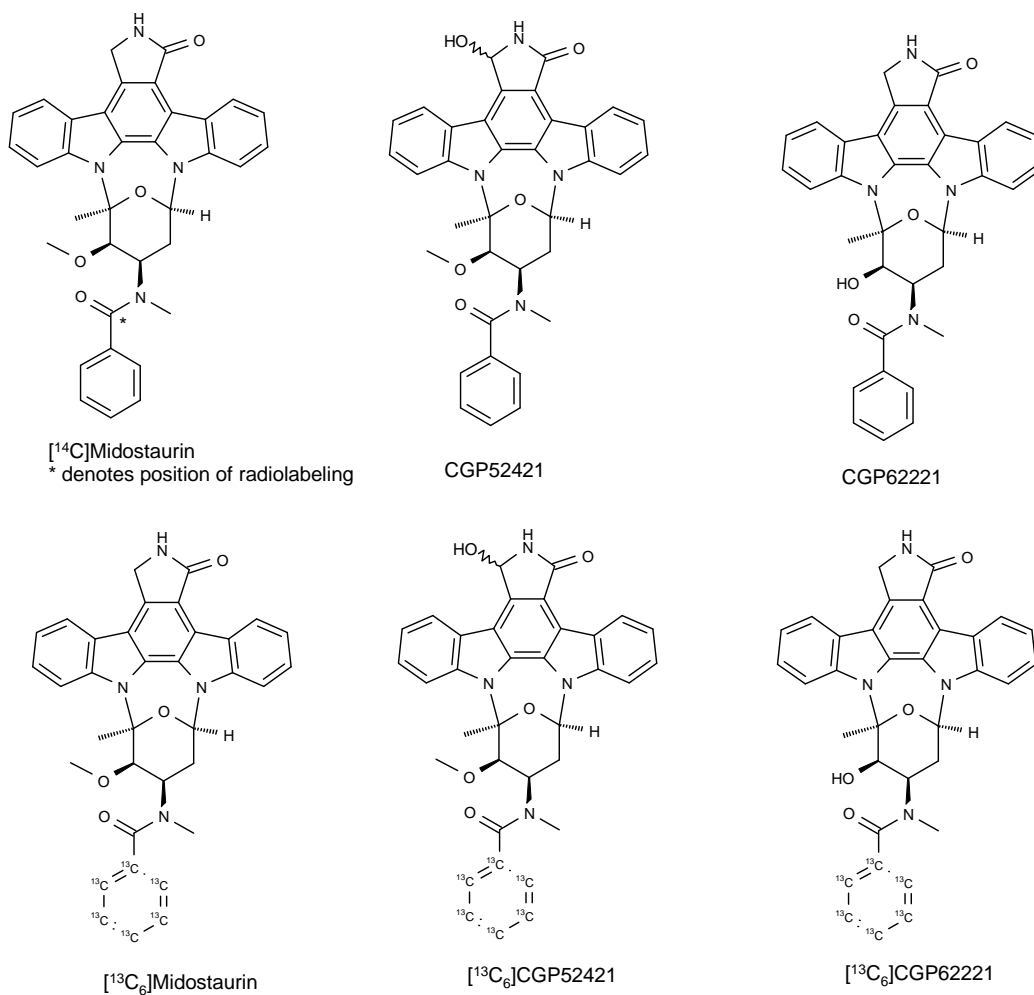


Figure 2

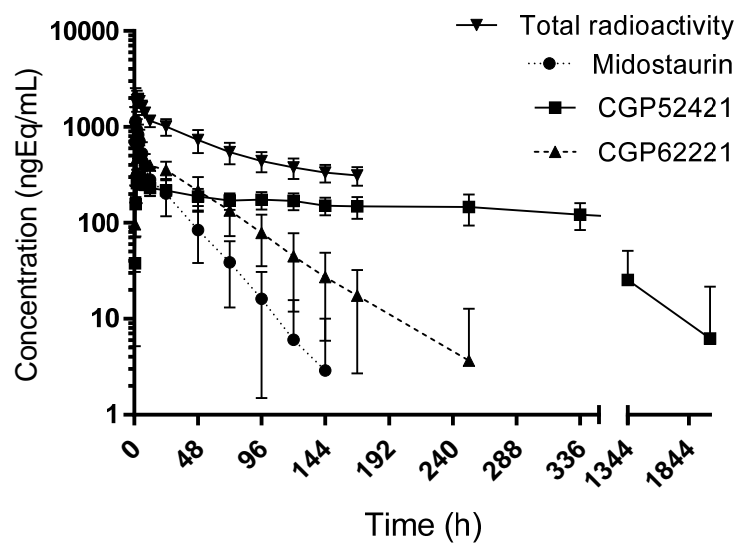


Figure 3

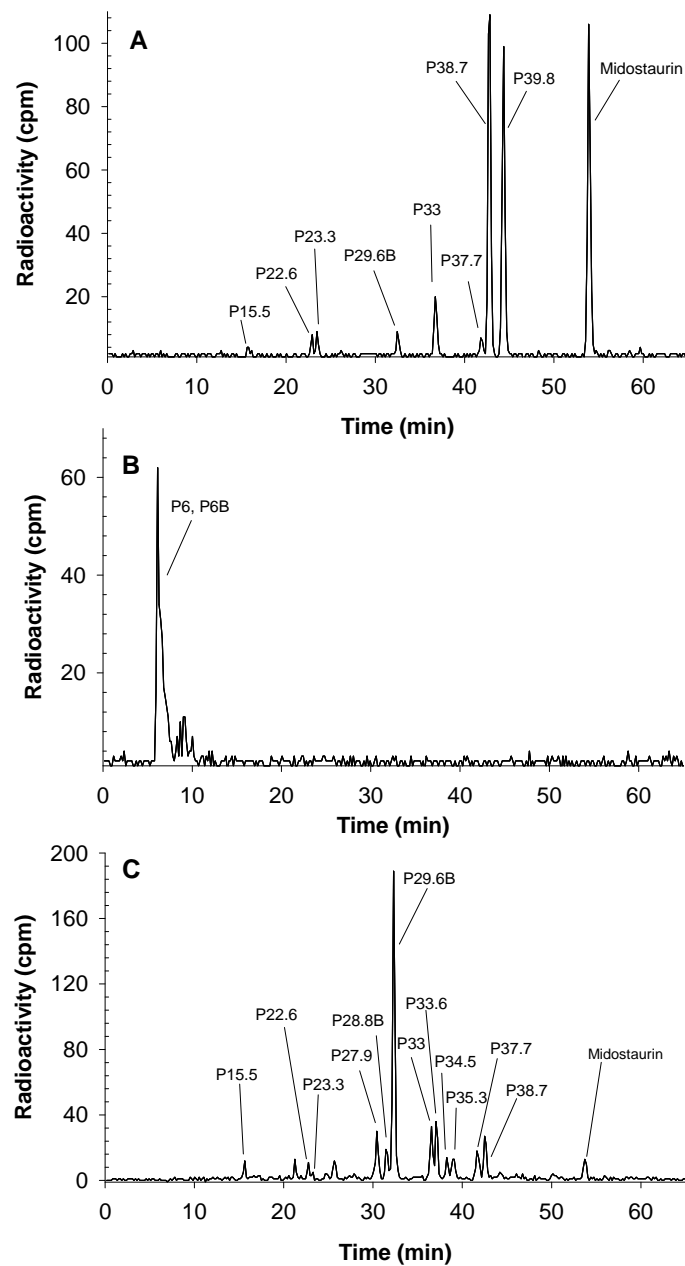




Figure 4

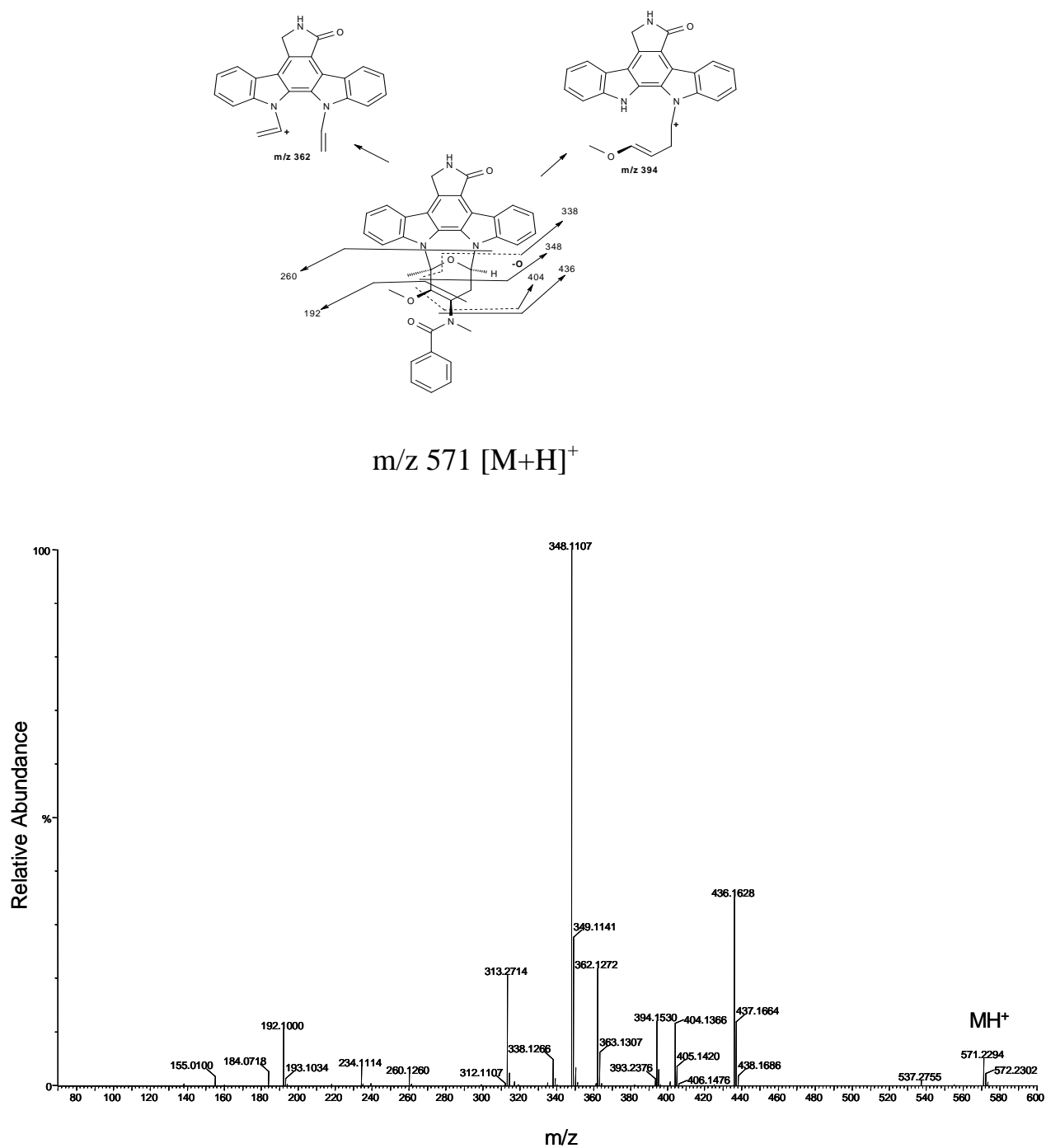


Figure 5

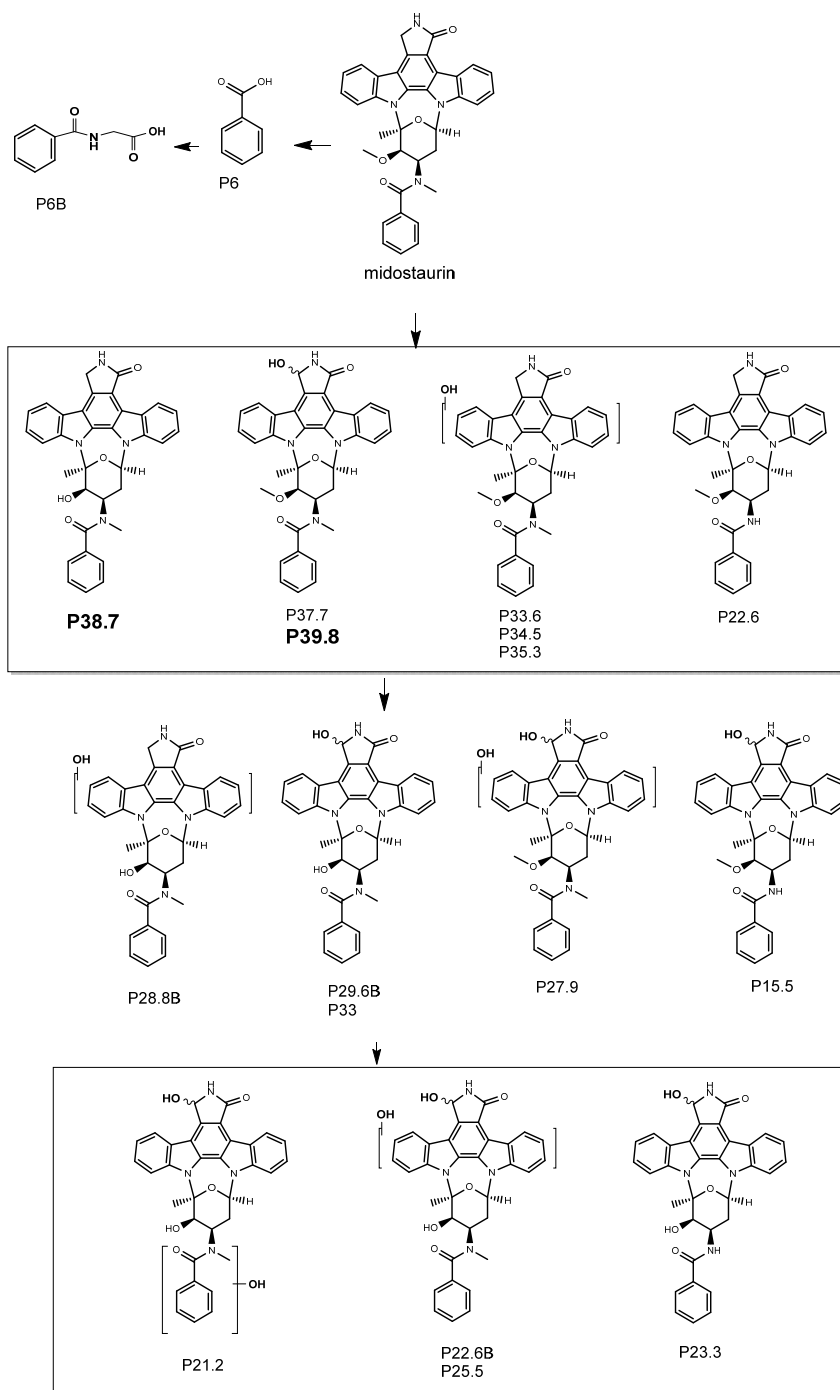


Figure 6

[<sup>14</sup>C] Midostaurin, 50 mg

